

## Body Force Circulation and the Antarctic Ozone Minimum

TIMOTHY J. DUNKERTON

*Northwest Research Associates, Inc., Bellevue, Washington*

(Manuscript received 20 April 1987, in final form 2 September 1987)

### ABSTRACT

The decelerating effect of enhanced upper tropospheric wavelike driving ( $D_F$ ) in winter and early spring induces a "reverse" component of the residual mean meridional circulation in the polar lower stratosphere opposite to that induced by radiative cooling. The cooling, in turn, is maintained by the decelerating effect of stratospheric  $D_F$ . If the upper-tropospheric wavelike driving is increased, and the stratospheric wavelike driving is sufficiently reduced, the change in the mean circulation will include upwelling in the polar lower stratosphere. Analytic and numerically derived properties of this generalized residual mean "body force" circulation are discussed.

### 1. Introduction

Interest in the dynamical meteorology of the polar lower stratosphere has heightened with the recently discovered interannual decline of spring seasonal minima in Antarctic total ozone (Farman et al., 1985; Bowman, 1986; Chubachi and Kajiwara, 1986; Gardiner and Shanklin, 1986; Bojkov, 1986; Komhyr et al., 1986). Correlation of total ozone with lower stratospheric temperatures has been reported on several time scales, including seasonal and interannual (Sekiguchi, 1986; Newman and Schoeberl, 1986; Schoeberl et al., 1986; Chubachi, 1986; Angell, 1986). Further, Stolarski and Schoeberl (1986) noted that the integrated total ozone south of 44°S does not undergo a seasonal decline towards spring, due to a compensating buildup in midlatitudes (although a midlatitude interannual decline was evident in their data). In view of the ozone-temperature correlation it is not surprising that in addition to chemical and aerosol-related theories of Antarctic ozone depletion (Solomon, 1987; Hofmann et al., 1987; and refs.), dynamical explanations involving a reversed mean meridional circulation have been advanced (Tung et al., 1986; Tung, 1986; Mahlman and Fels, 1986).

Interpretation of the ozone trends is complicated by the extreme meteorological conditions prevalent in the Antarctic lower stratosphere during winter and early spring. Compared to the northern winter polar stratosphere the Antarctic mean temperatures are climatologically 10–20 K colder (dropping below 190 K), the interhemispheric difference being the greatest as the spring equinox is approached due to the delayed final warming of the Southern Hemisphere (Geller et al.,

1984; Mechoso et al., 1985). Formation of polar stratospheric clouds has been attributed to these cold temperatures (e.g., Stanford, 1973, 1977; Stanford and Davis, 1974; McCormick and Trepte, 1986; Hamill et al., 1986). Also, the southern circumpolar vortex is less disturbed by planetary waves (Leovy and Webster, 1976; Hartmann, 1976; Labitzke, 1981; Barnett and Corney, 1985b). In contrast, winter tropospheric wave activity exists at a comparable level in both hemispheres (Mechoso et al., 1985; Shiotani and Gille, 1987; cp. Edmon et al., 1980; Geller et al., 1984; Baldwin et al., 1985).

Because of these extreme conditions it is uncertain what fraction of the Antarctic ozone depletion is dynamical or chemical in origin; the proposed dynamical and chemical theories are, in any case, interdependent. However, there is a dynamical mechanism important to the polar lower stratosphere of both hemispheres originating in the upper troposphere, which is relevant to the ozone problem, has not been discussed in the literature, and is relatively insensitive to the dynamics and composition of the stratosphere. First discussed in its general context by Eliassen (1951), the mechanism involves a "body force" circulation. (The quote marks are appropriate because we are discussing the source term in the zonal momentum equation of the transformed Eulerian mean system. In practice, a vertical divergence or convergence of meridional heat flux may be essential to this source term.) It may be explained in simplest terms as follows. The Eliassen-Palm flux convergence prevalent in the upper troposphere of winter and early spring drives a residual mean meridional wind component ( $\bar{v}^*$ ) towards the pole (Edmon et al., 1980). The average magnitude of this decelerating force per unit mass is 6–8 m s<sup>-1</sup>/day, in a broad but shallow band at 9 km (300–400 mb), maximizing between 50° and 75° latitude (Mechoso et al., 1985; Shiotani and Gille, 1987). [Somewhat higher values of

*Corresponding author address:* Dr. Timothy J. Dunkerton, Northwest Research Associates, Inc., P.O. Box 3027, Bellevue, WA 98009.

upper-tropospheric  $D_F$  were attained in the GFDL "SKYHI" model (Andrews et al., 1983; Miyahara et al., 1986).] The required Coriolis torque for a balance is achieved with  $\bar{v}^* \sim 0.6 \text{ m s}^{-1}$ . In polar latitudes, the residual vertical velocity difference corresponding to a meridional inflow of this magnitude, one scale height deep, decaying between  $60^\circ$  and the pole, is then  $\Delta\bar{w}^* \sim 0.14 \text{ cm s}^{-1}$ . The partition between upward and downward flow depends on several factors including the frequency and latitudinal structure of the forcing, mechanical and thermal damping rates, and static stability (Dunkerton, 1988). The calculations reported later in this paper indicate that a typical value of the upward component above 12 km is  $\bar{w}^* \sim 0.05 \text{ cm s}^{-1}$ .

In the northern polar lower stratosphere of winter and early spring, a residual vertical velocity of this magnitude would normally be opposed and overshadowed by radiative cooling. Horizontal constituent transport would also be affected by planetary wave-induced mixing on isentropic surfaces (Tung, 1982; Leovy et al., 1985). Considering the diabatic circulation per se we note from Dopplack (1979) that the total radiative cooling rate in the northern polar lower stratosphere of winter and spring is in the range  $0.3\text{--}1.0 \text{ K day}^{-1}$ , while the value in the southern polar lower stratosphere, six months later, is considerably lower: about  $0.1\text{--}0.5 \text{ K day}^{-1}$ . These numbers (including the sign of the latter) are uncertain on account of stratospheric composition and other factors; they do, however, suggest a closer approach of southern polar temperatures to radiative equilibrium, as expected.

In the northern winter stratosphere there is significant interannual variability closely tied to variations in planetary wave momentum and heat transport (Labitze, 1981; Smith, 1983; Geller et al., 1984). The integrated effect of the planetary waves is to decelerate the middle atmosphere flow, maintaining the polar stratospheric temperatures well above radiative equilibrium. It has been frequently pointed out (e.g., Mahlman et al., 1984) that the radiative cooling of the winter stratosphere responsible for the downward residual circulation of Dunkerton (1978) owes its existence to the decelerating effect of stratospheric planetary waves. This prompts the question as to how the circulation would respond if the stratospheric (tropospheric) waned driving  $D_F$  were significantly reduced (increased). The answer is apparently that the polar lower stratosphere would first approach radiative equilibrium, and then be driven to slightly colder temperatures by the upper-tropospheric  $D_F$ . This would result in local upwelling and positive total radiative heating. Although it may not be realistic carried to this extreme, this example illustrates how a change in waned driving can induce a "reverse" mean meridional circulation is therefore a consequence of enhanced upper-tropospheric waned driving, coupled with significantly reduced stratospheric planetary waned driving.

There are three observations that suggest a possible

explanation of the seasonal and interannual declines in temperature and column ozone in the Antarctic lower stratosphere. First, according to Fig. 5 of Mechoso et al. (1985), the region of maximum upper-tropospheric waned driving (convergent  $D_F$ ) drifts poleward between June and September (based on 1979–82 data). For example, near  $60^\circ\text{S}$  the monthly mean values are  $4\text{--}6 \text{ m s}^{-1}/\text{day}$  in June, increasing slightly to  $6\text{--}8 \text{ m s}^{-1}/\text{day}$  in September. Stratospheric waned driving also increases slightly during this time, but is confined above about 30 km. (Monthly mean  $D_F$  much larger than  $2 \text{ m s}^{-1}/\text{day}$ , commonly observed in the northern winter between 15 and 30 km, are apparently nonexistent in the southern lower stratosphere, where  $D_F$  seldom exceeds this value in this altitude range.) Second, upper-tropospheric monthly mean  $D_F$  for September has grown perhaps 10%–20% larger in 1983–85, according to Eliassen-Palm cross sections provided by C. R. Mechoso (personal communication, 1987). It was noted by W. J. Randel (personal communication, 1987) that zonal wavenumbers 3–8 were responsible for this increase. Third, with the exception of 1982 there has been a fairly steady decline in the September monthly mean vertical EP flux entering the stratosphere at 100 mb (Nagatani and Miller, 1987). Consistent with this, Mechoso's cross sections indicate that the upper-stratospheric waned driving in September 1985 was generally weaker than in any previous year since 1979.

This investigation was motivated by the consideration that, irrespective of any seasonal or interannual trend, upper-tropospheric waned driving can, in some cases, have a quantitatively significant far-field effect in the polar lower stratosphere. Accordingly, the purpose of this paper is to discuss theoretically the body force problem posed by Eliassen (1951) and its application to "generic" upper-tropospheric waned driving seen in the observed climatologies. Section 2 will briefly review the interhemispheric differences in the winter and early spring circulation, followed by a derivation of the elliptic equation governing the residual mean meridional streamfunction (section 3), discussion of its analytic solution properties in negligible shear (section 4), and a numerical solution using the observed August winds under the assumption of radiative equilibrium (section 5). The effect of diabatic heating is discussed in section 6.

The "partial solution" approach adopted here, made possible by the linear nature of the streamfunction equation under a geostrophic assumption, is complementary to most recent discussions of the residual circulation which calculate a "diagnostic" circulation directly from the thermodynamic equation, the observed temperature tendency, and a radiative code. This latter method gives an indirect estimate of the body force, if the mean flow tendency and shear are known. How well the results of the two approaches agree depends on the accuracy of observed  $D_F$  and calculated radiative

heating, and will determine, in the final analysis, how well we understand the dynamical and thermodynamical problems posed by the observations.

**2. Winter and early spring circulation**

The observed interhemispheric difference in zonal and monthly mean temperature in the polar lower

stratosphere translates into a difference in gradient winds, shown in Fig. 1. This figure was created using the geopotential data of Barnett and Corney (1985a), and the gradient wind balance equation

$$f\bar{u} + \frac{\bar{u}^2 \tan\theta}{a} + \bar{\phi}_y = 0 \quad (2.1)$$

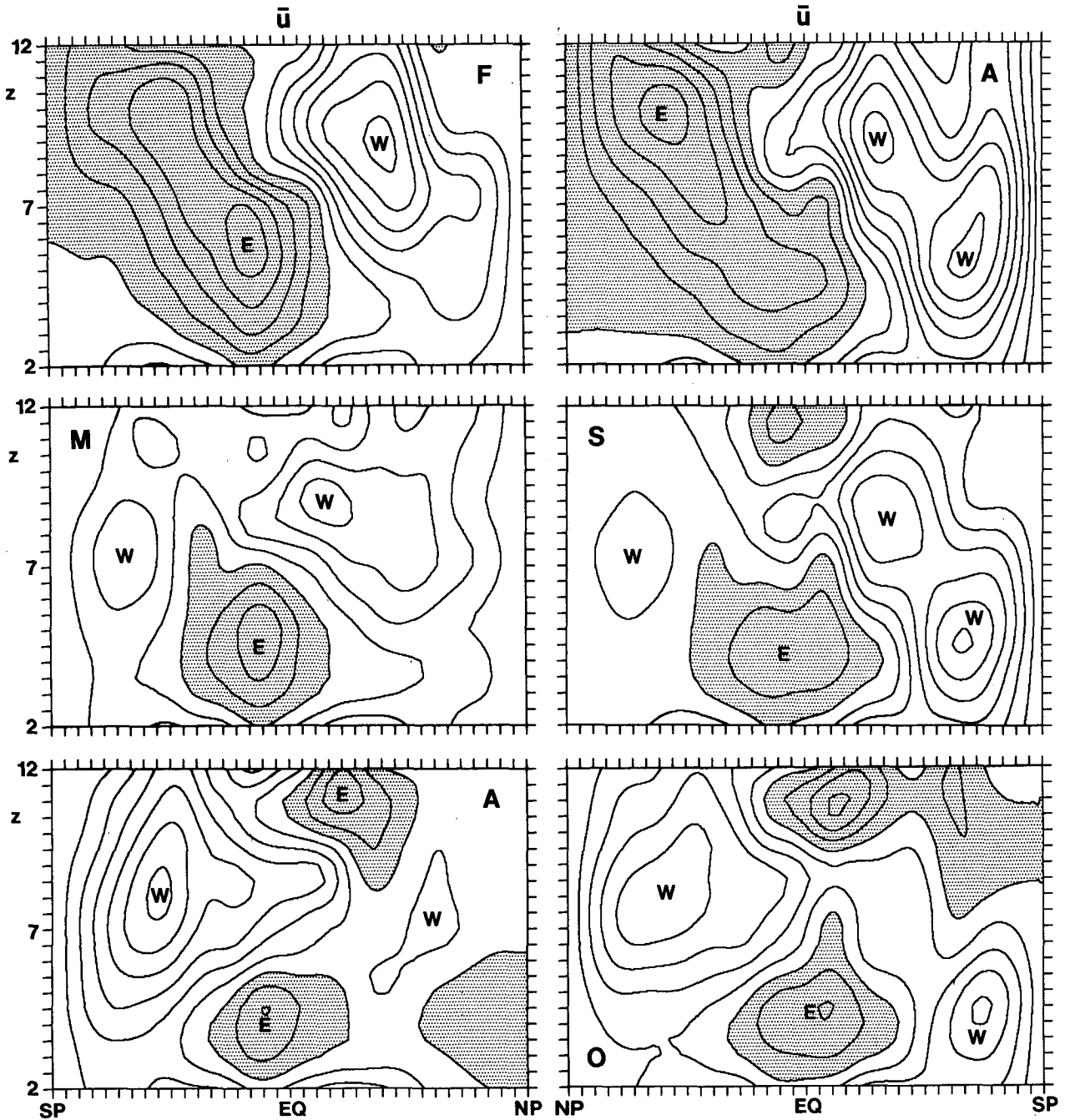


FIG. 1. Climatological gradient wind distribution for February–April (left) and August–October (right) calculated from geopotential data in Barnett and Corney (1985a) (see text). Vertical axis is in pressure scale heights, and the orientation of frames on the right has been reversed for easy comparison to those on the left. Contour interval is 10 m s<sup>-1</sup>, and easterly (negative) values are shaded. Linear interpolation was used between 80° and the pole, and between 10°N and 10°S.

where  $\bar{u}$  is zonal mean wind,  $f$  is the Coriolis parameter,  $\theta$  is latitude,  $\phi$  is zonal mean geopotential, and  $a$  is the radius of the earth. Values of gradient wind between  $80^\circ$  and the pole, and between  $10^\circ\text{N}$  and  $10^\circ\text{S}$ , were obtained by linear interpolation. The wind data were subsequently smoothed with a Fourier sine series in colatitude, truncated to 18 terms. In the figure, the vertical axis is labeled in pressure scale heights (about 7 km per scale height). Frames on the right-hand side were reversed in orientation for easy comparison to those on the left. The most striking difference is found in the polar lower stratosphere: the southern jet is much stronger, exceeding  $70 \text{ m s}^{-1}$ , in a region where corresponding speeds in the northern jet are only 20–30  $\text{m s}^{-1}$ . Note also that the effect of the gradient, as opposed to geostrophic, wind approximation has reduced the southern jet maximum from 90  $\text{m s}^{-1}$  (Barnett and Corney's August geostrophic wind maximum at  $70^\circ\text{S}$ ) to just above 70  $\text{m s}^{-1}$ . The maximum gradient winds agree somewhat better with the observed rocketsonde winds of Koshelkov (1985).

The northern and southern winter mean flows have similarities and differences in their potential vorticity gradient (not shown). Both have a region of reversed gradient in the winter tropical stratopause region, and another reversal on the poleward flank of the upper-level jet (Dunkerton and Delisi, 1985). The inter-hemispheric difference is more pronounced in the lower stratosphere, as expected. The southern polar night jet has a slightly negative potential vorticity gradient near  $40^\circ\text{S}$ , in agreement with Hartmann (1983). Insofar as this is true of the climatological average, individual daily or weekly mean distributions could be significantly negative in this region.

The importance of this reversed gradient region for stratospheric planetary waves is unclear, however. Theoretically, unstable barotropic normal modes are possible (Hartmann, 1983; Dunkerton, 1987). However, Mechoso and Hartmann (1982) also suggested that the traveling planetary waves of the southern winter stratosphere may be attributable to the "Green mode" of baroclinic instability (Geisler and Garcia, 1977; Straus, 1981; Zhang and Sasamori, 1985). For the purposes of a mean meridional circulation, the Eliassen-Palm cross sections of Mechoso et al. (1985) and Shiotani and Gille (1987) do not suggest any strong positive wavedriving in the stratosphere in the region of reversed potential vorticity gradient, at least not in a monthly or climatologically averaged sense. Instead, there is a prominent region of decelerating  $D_F$  in the upper troposphere.

As shown in section 5, the effect of these inter-hemispheric differences on an induced mean meridional circulation (given the same distribution of body forces or heating) is primarily through a change in absolute vorticity (which is higher poleward of the southern jet) and static stability (which is lower beneath the region of extreme cold temperature in the Antarctic lower stratosphere).

### 3. Residual mean meridional streamfunction

The transformed Eulerian mean equations for the zonally averaged flow (Andrews and McIntyre, 1976, 1978; Boyd, 1976), written in log-pressure coordinates (Holton, 1975) are

$$\bar{u}_t + \bar{v}^* \left( \frac{1}{\cos\theta} \frac{\partial}{\partial y} \bar{u} \cos\theta - f \right) + \bar{w}^* \bar{u}_z = D_F \quad (3.1a)$$

$$f\bar{u} + \frac{\bar{u}^2 \tan\theta}{a} + \bar{\phi}_y = 0 \quad (3.1b)$$

$$\bar{\phi}_{zi} + \bar{v}^* \bar{\phi}_{zy} + \bar{w}^* (N^2 + \bar{\phi}_{zz}) = \bar{Q}^* \quad (3.1c)$$

$$\frac{1}{\cos\theta} \frac{\partial}{\partial y} (\bar{v}^* \cos\theta) + \frac{1}{\rho_0} \frac{\partial}{\partial z} (\rho_0 \bar{w}^*) = 0 \quad (3.1d)$$

where  $\bar{v}^*$  and  $\bar{w}^*$  are meridional and vertical residual mean velocity,  $N^2$  is the buoyancy frequency squared,  $\rho_0$  is basic state density  $\rho_s \exp(-z/H)$ , and the gradient wind approximation has been made in (3.1b). The "body force" per unit mass is the Eliassen-Palm flux divergence factor

$$D_F = \frac{\nabla \cdot \mathbf{F}}{\rho_0 \cos\theta} \quad (3.2a)$$

where  $\mathbf{F}$  is the Eliassen-Palm flux (Dunkerton et al., 1981). The diabatic heating term is

$$\bar{Q}^* = \bar{Q} - \frac{1}{\rho_0} \frac{\partial}{\partial z} \rho_0 \left( \overline{w'\phi'_z} + \frac{\overline{v'\phi'_z \bar{\phi}_{zy}}}{N^2} \right) \quad (3.2b)$$

where  $\bar{Q}$  is the Eulerian mean diabatic heating.

A relation analogous to Eq. (5.7) of Holton (1975) is obtained by eliminating the time tendency from these equations, after making the geostrophic approximation in (3.1b) and defining a residual mean meridional streamfunction

$$\left( \frac{\partial}{\partial z} - \frac{1}{H} \right) \bar{\chi}^* = -\bar{v}^* \cos\theta \quad (3.3a)$$

$$\frac{\partial \bar{\chi}^*}{\partial y} = \bar{w}^* \cos\theta \quad (3.3b)$$

leading to

$$\begin{aligned} & f \left( f - \frac{1}{\cos\theta} \frac{\partial}{\partial y} \bar{u} \cos\theta \right) \left( \frac{\partial}{\partial z} - \frac{1}{H} \right) \frac{\partial \bar{\chi}^*}{\partial z} \\ & + f \bar{u}_z \left( 2 \frac{\partial}{\partial z} - \frac{1}{H} \right) \frac{\partial \bar{\chi}^*}{\partial y} \\ & + (N^2 + \bar{\phi}_{zz}) \cos\theta \frac{\partial}{\partial y} \left( \frac{1}{\cos\theta} \frac{\partial \bar{\chi}^*}{\partial y} \right) \\ & + O(2\Omega \bar{u}_z \bar{v}^*/a) = \cos\theta \left( f \frac{\partial D_F}{\partial z} + \frac{\partial \bar{Q}^*}{\partial y} \right) \quad (3.4) \end{aligned}$$

Equation (3.4) is elliptic provided that the Richardson number is larger than the ratio of planetary to absolute vorticity (Holton, 1975); the flow is assumed to be centrifugally and statically stable. This is a diagnostic

equation in the sense that, given the distribution of body forces and heating, the mean meridional circulation is calculable from (3.4) together with the boundary conditions on  $\bar{\chi}^*$  at the edge of the domain. The flow, however, is not steady except for special combinations of  $D_F$  and  $\bar{Q}^*$ . Equation (3.4) is also a linear equation, allowing a partial solution to be obtained for each component of  $D_F$  and  $\bar{Q}^*$ .

**4. Analytic solution in negligible shear**

Analytic or simple numerical methods may be used to solve (3.4) when terms involving  $\bar{u}$  are neglected and  $|\bar{\phi}_{zz}| \ll N^2$ . This problem was studied in various ways by Eliassen (1951), Leovy (1964), Matsuno and Nakamura (1979), Plumb (1982), Garcia (1987) and Dunkerton (1988). It is convenient to define

$$\mu = \sin\theta \tag{4.1a}$$

$$d\mu = \cos\theta d\theta \tag{4.1b}$$

$$f = 2\Omega\mu \tag{4.1c}$$

$$Z = z/H \tag{4.1d}$$

$$R = \left(\frac{NH}{2\Omega a}\right)^2 \tag{4.2}$$

$$F = \frac{HD_F}{2\Omega} \tag{4.3a}$$

$$Q = \frac{H^2\bar{Q}^*}{4\Omega^2 a} \tag{4.3b}$$

so that (dropping the overbar and asterisk)

$$\left(\frac{\partial}{\partial Z} - 1\right) \frac{\partial \chi}{\partial Z} + R \frac{1 - \mu^2}{\mu^2} \frac{\partial^2 \chi}{\partial \mu^2} = \frac{\sqrt{1 - \mu^2}}{\mu} \frac{\partial F}{\partial Z} + \frac{1 - \mu^2}{\mu^2} \frac{\partial Q}{\partial \mu} \tag{4.4}$$

The dependent variable  $\chi$ , and forcing terms  $F, Q$ , may be expanded as

$$\begin{Bmatrix} \chi \\ F \\ Q \end{Bmatrix} = \sum_n \begin{Bmatrix} \chi_n(Z) \\ F_n(Z)\mu/\sqrt{1 - \mu^2} \\ Q_n(Z) \frac{\partial}{\partial \mu} \end{Bmatrix} \eta_n(\mu) \tag{4.5}$$

where

$$\eta_n''(\mu) \equiv \frac{\epsilon_n \mu^2}{1 - \mu^2} \eta_n(\mu) \tag{4.6a}$$

$$\eta(\pm 1) \equiv 0. \tag{4.6b}$$

The expansion of  $F$  in (4.5) requires that (Plumb, 1982)

$$\lim_{\mu \rightarrow 0} F(\mu, Z) = O(\mu) \tag{4.7}$$

which is also a requirement for linear steady state solutions at the equator (cf. 3.1a). It is easily shown from (4.6a, b) that

$$(\epsilon_n - \epsilon_m) \int_{-1}^1 \frac{\mu^2}{1 - \mu^2} \eta_n \eta_m d\mu = 0 \tag{4.8a}$$

so that if  $\epsilon_n \neq \epsilon_m$ ,  $\eta_n$  and  $\eta_m$  are orthogonal. Also,

$$\epsilon_n^{-1} = - \int_{-1}^1 \frac{\mu^2}{1 - \mu^2} (\eta_n)^2 d\mu / \int_{-1}^1 (\eta_n')^2 d\mu < 0. \tag{4.8b}$$

The vertical structure equation obtained by inserting the series (4.5) into (4.4) is

$$\chi_n'' - \chi_n' + R\epsilon_n \chi_n = F_n' + \epsilon_n Q_n \tag{4.9}$$

(Leovy, 1964; Matsuno and Nakamura, 1979; Plumb, 1982). Solutions of the homogeneous problem (rhs of 4.9 set to zero) have an inverse decay scale  $\lambda_n$  such that

$$\chi_n \propto \exp \lambda_n Z \tag{4.10a}$$

$$\lambda_n = \frac{1}{2} \pm \left\{ R|\epsilon_n| + \frac{1}{4} \right\}^{1/2} \tag{4.10b}$$

(Plumb, 1982).

The homogeneous problem is relevant to localized forcings (Eliassen, 1951; Matsuno and Nakamura, 1979). For instance, if

$$F_n = \delta(z - z_c) \tag{4.11a}$$

$$Q_n = 0, \tag{4.11b}$$

define

$$g_n' = \chi_n \tag{4.12}$$

so that

$$g_n'' - g_n' + R\epsilon_n g_n = \delta(z - z_c). \tag{4.13}$$

The solution is obtained by matching two homogeneous solutions at  $z = z_c$ . The meridional velocity is singular at this level, with a return flow above and below (see Matsuno and Nakamura, 1979, for remaining details of their beta-plane case). The point source problem of Eliassen (1951) is more straightforward: set  $\tan\theta \sim 1$  in (4.4), neglect terms like  $1/H$ , and define  $Y = \mu R^{-1/2}$ , so that

$$\chi_{ZZ} + \chi_{YY} = \frac{\partial F}{\partial Z} \tag{4.14}$$

The solution is

$$\chi(\mathbf{x}) = \iint G(\mathbf{x} - \mathbf{x}') \frac{\partial F}{\partial Z'}(\mathbf{x}') d\mathbf{x}' \tag{4.15a}$$

where  $G$  is the Green's function

$$G(\mathbf{x} - \mathbf{x}') = \frac{1}{2\pi} \ln|\mathbf{x} - \mathbf{x}'| \tag{4.15b}$$

Integrating (4.15a) by parts, and setting  $F = \delta(\mathbf{x} - \mathbf{x}_0)$ ,

$$\chi(\mathbf{x}) = \frac{\partial}{\partial Z} G(\mathbf{x} - \mathbf{x}_0). \tag{4.16}$$

If the delta function is smeared slightly about the point  $\mathbf{x}_0$ , the circulation shown schematically in Fig. 2a is obtained. The Coriolis torque opposes the point source at that level (analogous to Lenz' law) but has the same

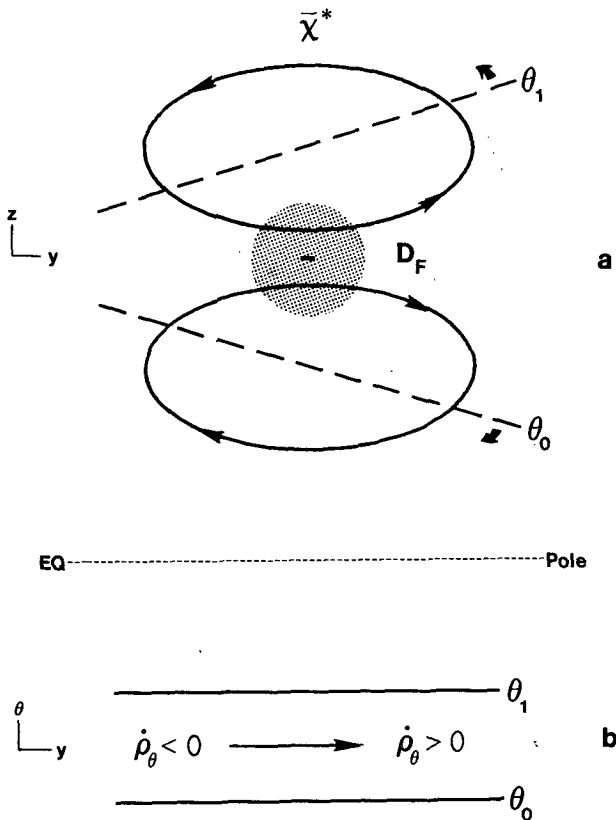


FIG. 2. Schematic illustration of the body-force circulation induced by a locally negative wavedriving  $D_F$ . In the lower panel, the same process is visualized in isentropic coordinates.

sign as  $D_F$  in the return branches above and below the point source. Relative to  $D_F$ , the net acceleration is compressed horizontally and extended vertically (Dunkerton et al., 1981; Dunkerton and Delisi, 1985).

Because the motion is adiabatic, the isentropic or potential temperature ( $\theta$ ) surfaces are tilted by the circulation. In isentropic coordinates (Fig. 2b) the isentropic "density"

$$\rho_\theta \equiv \rho \frac{\partial z}{\partial \theta} \quad (4.17)$$

increases (decreases) poleward (equatorward) of the point source, because there is more (less) mass between isentropic surfaces as time progresses.

Returning to the general problem on the sphere (4.6, 10), the vertical decay scale depends on  $n$ ,  $\epsilon_n$  and  $R$ . Values of  $\lambda_n^{-1}$  together with eigenvalues for the first 12 eigenfunctions are shown in Table 1. These were obtained with a finite-difference shooting algorithm applied to (4.6) with  $\Delta\mu = 0.001$ . (The higher resolution than that of Plumb gave better agreement to Leovy's eigenvalues.) The value of  $R$  was taken to be 0.02276, corresponding to  $N = 0.02 \text{ s}^{-1}$ ,  $a = 6.37 \times 10^6 \text{ m}$ ,  $\Omega = 7.29 \times 10^{-5} \text{ s}^{-1}$ , and  $H = 7 \text{ km}$ . The vertical decay scale is given in scale heights. In addition to the solution

properties cited above, the eigenvalues of Table 1 and their corresponding eigenfunctions have the following characteristics. First, the upward-decaying solutions have a much larger scale, particularly for the lowest  $n$ . The vertical extent is exaggerated above the level of forcing due to atmospheric quasi-compressibility. Second, the eigenvalues come (approximately) in pairs. Third, odd and even values of  $n$  have corresponding eigenfunctions which are symmetric (antisymmetric) about the equator, and are easily related to the Hough function solutions of the zonally symmetric Laplace tidal equation (Plumb, 1982). The reader is referred to Plumb's paper for their structure. A novel aspect of these eigenfunctions discovered in the present investigation was motivated by the pairing of adjacent odd and even eigenvalues. Figure 3 shows the first three eigenfunction pairs, obtained by adding together equal amounts of odd and even functions normalized according to

$$\bar{\eta}_n \equiv \frac{\eta_n}{\max(\eta_n)} \quad (4.18)$$

The interesting aspect of Fig. 3b is that the combinations representing the body force  $F$  are confined to one hemisphere (to within about 20%). If the total body force is confined to one hemisphere, and is zero at the equator as in (4.7),  $F$  might be crudely expanded in terms of these combined eigenfunctions. The degree to which the streamfunction will penetrate across the equator is then evident from Fig. 3a. Table 1 suggests that the lowest values of  $n$  will dominate far above the level of forcing, for which the cross-equatorial penetration is easily estimated.

## 5. Body force circulation

To investigate streamfunction solutions in realistic shear, Eq. (3.4) was written in finite-difference form on a sine (latitude) grid extending from pole to pole (37 points) and from the surface to 42 km (43 points). The diabatic heating term was set to zero, and the body force term was assigned an analytic form resembling

TABLE 1. Eigenvalues and related vertical scales (in scale heights) of the first 12 eigenfunctions for  $R = 0.02276$ .

$n$	$-\epsilon_n$	$\lambda_n^{-1} (+)$	$\lambda_n^{-1} (-)$
1	8.127	.862	-6.27
2	12.54	.812	-4.32
3	35.42	.655	-1.90
4	44.73	.615	-1.60
5	82.38	.511	-1.04
6	96.62	.484	-.939
7	149.1	.415	-.710
8	168.2	.397	-.658
9	235.5	.349	-.535
10	259.6	.335	-.505
11	341.6	.300	-.429
12	370.7	.290	-.409

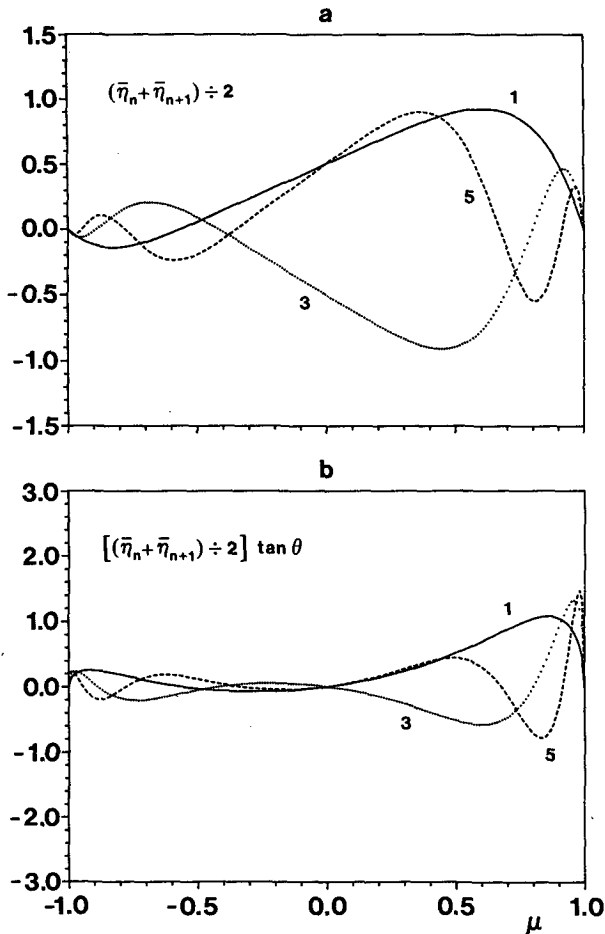


FIG. 3. Combinations of odd and even eigenfunctions to Eq. (4.6), made by adding together two adjacent eigenfunctions normalized to the same maximum amplitude. The lower panel is relevant to the functional expansion of body force  $F$ , provided that  $F$  vanish at the equator in accord with (4.7).

the 4-month, 4-year climatological average wavedriving given in Mechoso et al. (1985):

$$D_F = (-8 \times 10^{-5} \text{ m s}^{-2}) \cdot (S_1 - rS_2) \quad (5.1a)$$

$$S_1 = \left[ 1 - \left( \frac{\theta + \pi/3}{\pi/6} \right)^2 \right]^{1/2} \left[ 1 - \left( \frac{z - 9 \text{ km}}{4.5 \text{ km}} \right)^2 \right],$$

$$\begin{cases} -\frac{\pi}{2} \leq \theta \leq -\frac{\pi}{6} \\ 4.5 \leq z \leq 13.5 \text{ km} \end{cases} \quad (5.1b)$$

$$S_2 = \left[ 1 - \left( \frac{\theta + \pi/4}{\pi/12} \right)^2 \right] \left[ 1 - \left( \frac{z}{4.5 \text{ km}} \right)^2 \right],$$

$$\begin{cases} -\frac{\pi}{3} \leq \theta \leq -\frac{\pi}{6} \\ 0 \leq z \leq 4.5 \text{ km}. \end{cases} \quad (5.1c)$$

The value  $r = 0.7961$  was chosen to make the volume-integrated (density and  $\cos^2$  weighted)  $D_F$  vanish. The analytic profile of  $D_F$  together with the resulting streamfunctions are shown in Fig. 4a-c. The sine (latitude) coordinate is retained on the lower axis (having the effect of compressing most of the Antarctic continent to within one grid box). In Fig. 4b, the August climatological average gradient wind profile from Barnett and Corney (1985a) was used (Fig. 1), with tropospheric values obtained by linear interpolation. In Fig. 4c,  $\bar{u}$  was set to zero.

The intense, closed circulation of the troposphere is accompanied by a reverse circulation in the lower stratosphere, with upwelling at the pole of about  $0.04\text{--}0.06 \text{ cm s}^{-1}$  in Figs. 4b and c, respectively. The quantitative difference between the two figures seems to arise mainly on account of the increased vorticity of the circulation poleward of the August jet maximum. Both figures are significantly influenced by the static stability profile, which was taken to be

$$N = \begin{cases} 0.025 \text{ s}^{-1}, & z > 25 \text{ km} \\ 0.015 \text{ s}^{-1} + 0.010 \text{ s}^{-1}(z - 9 \text{ km})/16 \text{ km} \\ 0.015 \text{ s}^{-1}, & z < 9 \text{ km} \end{cases} \quad (5.2)$$

independent of latitude. Higher values of  $N^2$  (like the product of planetary and absolute vorticity) act to reduce the streamfunction magnitude [cf. (3.4)]. Both effects are intuitively reasonable since the higher stratification may be thought to oppose vertical motion, while a higher absolute vorticity requires less meridional flow to achieve the same Coriolis torque.

The analytic results of the preceding section are helpful in interpreting the numerical solutions. The body-force profile projects significantly onto the lowest-order modes (cp. Figs. 3b and 4a). As a result, the vertical decay scale is quite large. Indeed, it is possible that the truncated vertical domain (42 km) artificially compressed the solution somewhat (having negligible effect on vertical velocities just above the source region).

A more fundamental point is that the reverse circulation in the lower stratosphere exists despite the dipole structure of tropospheric  $D_F$  because the upper-tropospheric source is closer to the stratosphere than the lower-tropospheric source (in accord with the simple result of Eliassen previously cited). The upper-tropospheric source is also of slightly larger magnitude and broader latitudinal extent. Incidentally, the lower-boundary condition on  $\bar{\chi}^*$  was set to zero, requiring zero vertical EP flux at the boundary and no Eulerian mean vertical motion there (i.e.,  $dp/dt = 0$ ). In general, the EP flux is nonzero at the lowest standard level (1000 mb) appearing in EP cross sections. Thus, the residual streamlines could intersect the lower boundary (Edmon et al., 1980). Conceptually, it is easier to assume that  $\bar{\chi}^* \equiv 0$  at  $z = 0$ , and to insert an infinitesimally thin boundary layer between the ground and the lowest level

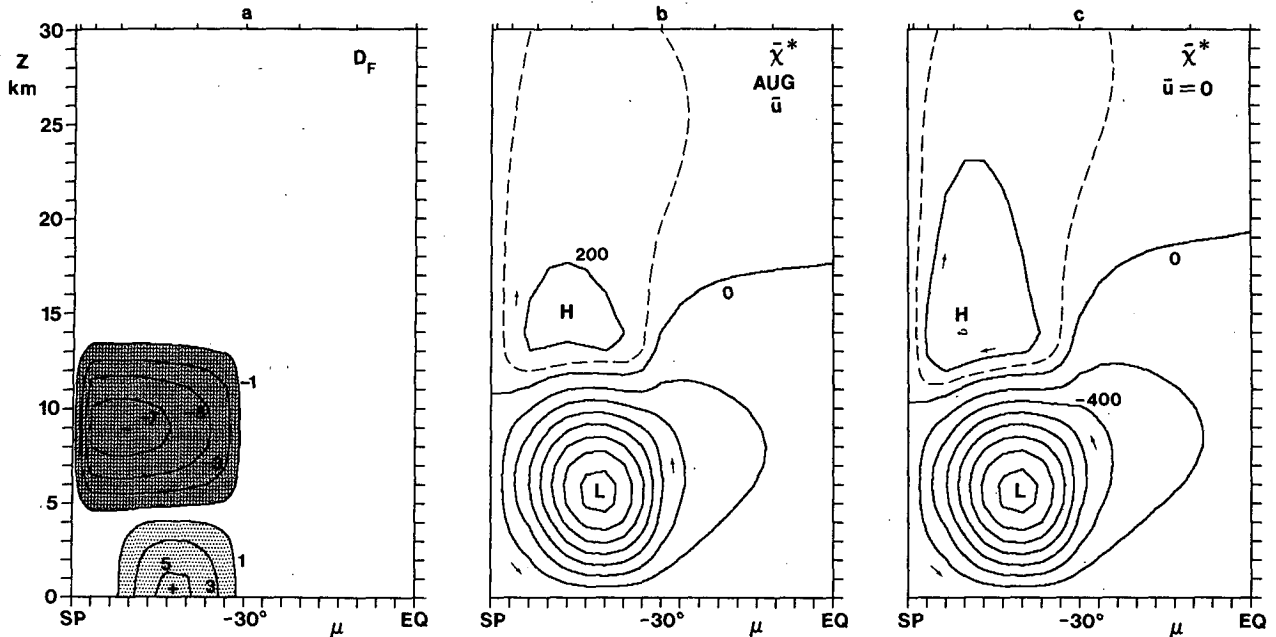


FIG. 4. (a) Body force per unit mass  $D_F$  used in the numerical solution of (3.4) with (b) August climatological gradient winds and (c)  $\bar{u} = 0$ . Contour interval in (a) is  $10^{-5} \text{ m s}^{-2}$  (zero contour not shown). In (b), the contour interval for residual mean meridional streamfunction is  $200 \text{ m}^2 \text{ s}^{-1}$ . Note that the vertical velocity is easily estimated on the sine latitude grid using (3.3b).

at which the EP flux is considered to be nonzero (i.e., comparable to its value in the free atmosphere). In this case the EP flux might be infinitely divergent at the top of the boundary layer. For the problem considered by Eliassen (1951) the solution is found by inserting an image point source beneath the surface at  $x_0^i = (y_0, -z_0)$ . If the point source is at the surface, its image is at the same point, and the circulation is of the same shape and orientation as before (see Eliassen's Fig. 14).

In the present example, the lower-tropospheric wavelike driving resembles a smeared-out delta function. If it were instead concentrated near the surface, with the same integrated magnitude, the far-field solution in the lower stratosphere would not be expected to change significantly. However, no attempt has been made to take into account the topographic influence of the Antarctic continent in the boundary condition.

It might be noted from Mechoso et al. (1985) that the lower-tropospheric wavelike driving changes significantly from month to month and from year to year. Its value may even be sensitive to the method by which the divergence factor is computed at the lower boundary. For the present purpose this variability is of secondary importance, except in one respect. For the proposed upwelling mechanism to be significant, it is essential that the upper-tropospheric wavelike driving extend nearer to the pole than the lower-level wavelike driving, as in Fig. 4a. Subsequent calculations indicated that, if the lower-level wavelike driving was assigned the same latitudinal structure as at upper levels, the net upward residual vertical velocity in the polar lower stratosphere could be reduced to less than half its value shown in Figs. 4b, c (not shown).

## 6. Diabatic effects

The circulation shown in Fig. 4b, c predicts only the initial tendency beginning from a state of radiative equilibrium (more precisely,  $\bar{Q}^* = 0$ ). Once the isentropic surfaces are displaced by the circulation, the atmosphere will no longer be in radiative balance. Constituents responsible for the radiative heating/cooling will also be displaced by the circulation. Thus, even though the streamfunction equation is linear, and can be solved in terms of partial solutions, many of the individual forcing components are coupled together. Moreover, it is apparent from our discussion thus far that some of these components are comparable in magnitude, and of opposite sign, making for a delicate balance of terms in the Antarctic lower stratosphere.

Several qualitative aspects of the flow evolution in the presence of radiative heating can be elucidated with a simple linear model based on the material reviewed in section 4. Namely, if

$$\frac{\partial \bar{T}}{\partial t} + \frac{HN^2}{R_g} \bar{w}^* = \bar{J} = \alpha(\bar{T}^E - \bar{T}) \quad (6.1a)$$

with constant  $\bar{T}^E$ ,  $\alpha$  then the time-dependent linear thermodynamic equation is simply

$$\left( \frac{\partial}{\partial t} + \alpha \right) \bar{J} = \frac{HN^2}{R_g} \alpha \bar{w}^* \quad (6.1b)$$

with  $\bar{w}^*$  given by the solution of (4.4) subject to a specified  $D_F$  and boundary conditions ( $R_g$  is the gas constant). The expansion of  $\bar{J}$  has been given in (4.5). The heating  $\bar{J}$ , like  $D_F$ , is subject to certain restrictions if completeness is required in terms of the basis set  $\eta_n$ :

$$\int_{-1}^1 \bar{J}(\mu) d\mu = 0 \quad (6.2a)$$

$$\lim_{\mu \rightarrow 0} \frac{\partial \bar{J}}{\partial \mu} = O(\mu^2) \quad (6.2b)$$

For each component, the evolution equation is

$$\left( \frac{\partial}{\partial t} + \alpha \right) J_n = \frac{HN^2}{R_g a} \alpha \chi_n \quad (6.3)$$

together with (4.9) and vertical boundary conditions.

This linear equation set has been solved for some simple cases using a specified, temporally constant  $D_F$  profile and an initial condition on  $J_n$ , namely

$$J_n = \alpha(T_n^E - T_n) = \alpha T_n^E \quad (6.4)$$

where

$$T_{1,2}^E = 10 \text{ K } (-)^n \text{ if } z > 10 \text{ km} \quad (6.5a)$$

$$\alpha(z) = \alpha_S(z) + \alpha_T(z) \quad (6.5b)$$

$$\alpha_S(z) = \left\{ .07 + .06 \tanh \frac{z-35}{10 \text{ km}} \right\} d^{-1} \quad (6.5c)$$

$$\alpha_T(z) = \left\{ .07 - .07 \tanh \frac{z-8}{1 \text{ km}} \right\} d^{-1} \quad (6.5d)$$

Orthonormal  $\eta_n$  were used in (6.5a) such that for  $z > 10 \text{ km}$ ,

$$\bar{T}^E(-1, z) \approx -43 \text{ K} \quad (6.5e)$$

(relative, not absolute, temperature), with  $\bar{T}^E$  mainly confined to one hemisphere by analogy to Fig. 3. The

implied heating at the south pole, for example, was initially

$$\bar{J}(-1, 15 \text{ km}) \approx -5 \text{ K } d^{-1} \quad (6.5f)$$

increasing with height. The rapid, artificial tropospheric relaxation in (6.5d) was used to hold the troposphere to quasi-steady conditions as observed in the Antarctic winter. Vertical boundary conditions were

$$\chi_n(0) = 0; \quad \chi'_n(42 \text{ km}) = 0 \quad (6.6)$$

and (4.9) was solved with 43 grid points. Twelve  $\eta_n$  functions were used in the horizontal representation (adequate for the Fig. 4 solution). The stability profile was given by (5.2).

Figure 5 shows the streamfunction and heating profiles at the 15 km level, at 30 day intervals, for three cases.

- Case I: no wavedriving
- Case II:  $D_F$  as in Fig. 4a
- Case III: modified  $D_F$  profile.

The modified  $D_F$  profile was similar to (5.1) except that the latitudinal structure function in (5.1b) was replaced by the corresponding function in (5.1c), making the two identical (with  $r = 0.5987$ ). A  $D_F$  profile of this type might be associated with a strictly vertical EP flux confined to midlatitudes.

There is nothing particularly interesting about Case I: the flow relaxes to radiative equilibrium, and in high latitudes is opposed by the descending branch of a mean meridional circulation that decays with time. This example illustrates, nevertheless, that under the assumed conditions, a quasi-conservative vertically stratified

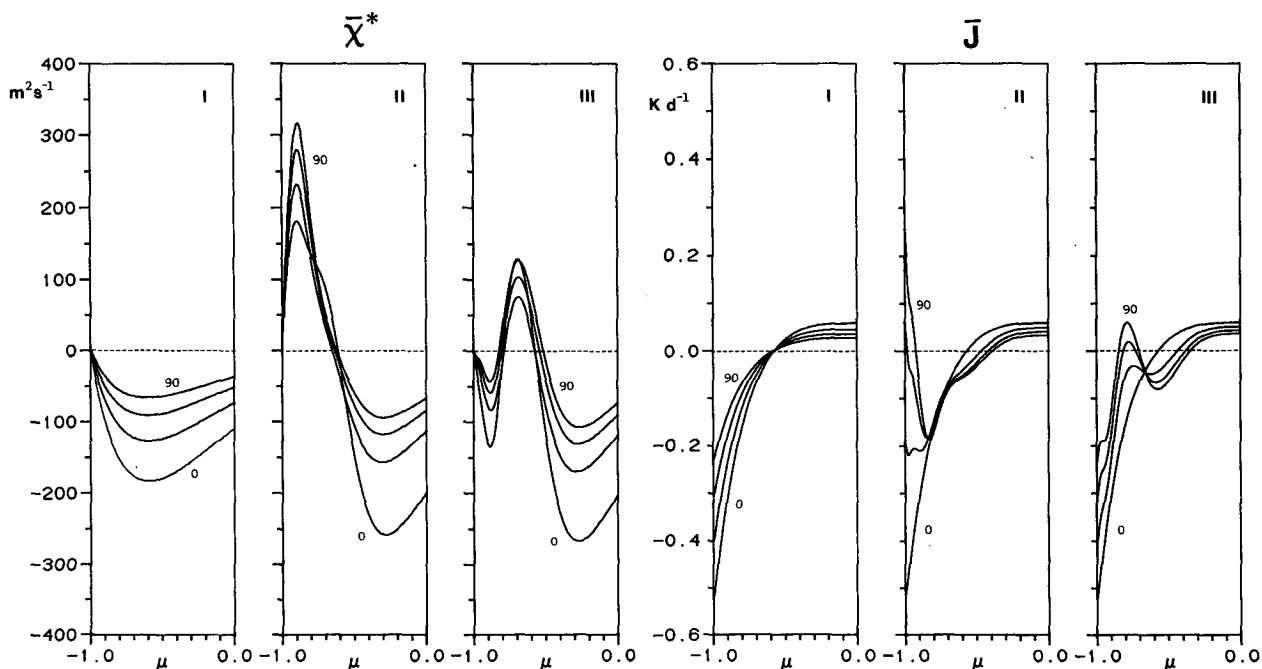


FIG. 5. Time-dependent evolution of streamfunction and diabatic heating for the simple experiments described in section 6. Latitudinal profiles at 15 km are shown at 30 day intervals.

tracer will have its isolines displaced downward in the presence of radiative cooling, the greatest downward displacement occurring at the pole.

Case II demonstrates the main theme of this paper, that the tropospheric wavelike driving in Fig. 4a induces a mean meridional circulation with upwelling in the polar lower stratosphere comparable to, and in this case greater than, the opposing diabatically induced subsidence. In this region the subsidence decays with time, giving way to stronger net upwelling and positive heating as temperatures are driven below radiative equilibrium. This trend could not continue indefinitely to a finite steady state unless the boundary conditions were changed.

Case III illustrates the caution flag raised at the end of the previous section: the instantaneous as well as steady-state circulations depend sensitively on the relative magnitude and alignment of the upper and lower-tropospheric momentum sources. In Case III, the circulation in the polar lower stratosphere induced by  $D_F$  alone is weaker than in Case II, and is overwhelmed by the initial diabatic circulation. A smaller reverse cell is confined to the midlatitude lower stratosphere in this case. The steady-state solution collapses to zero above the uppermost momentum source (not shown).

These illustrative examples might be generalized. The radiative heating could be coupled to the relevant constituent fields advected by the circulation, irreversible photochemical effects could be included, and the momentum sources (including stratospheric wavelike driving) made to vary with the evolving mean flow. These generalizations are outside the scope of the present paper.

In relating these simple results to the newly popular Antarctic ozone "hole", two crucial points will need to be addressed. It is uncertain, first of all, whether absolute upward motion at the pole is consistent with aerosol and  $N_2O$  observations. These observations are inconclusive because the aerosol sedimentation rate and tropospheric  $N_2O$  distributions are not yet known (Solomon, 1987). If upwelling is ruled out, the role of tropospheric wavelike driving might contribute to a differential effect<sup>1</sup> whereby midlatitude temperatures are

held further from radiative equilibrium than polar temperatures, as implied by Doplick (1979) and, more recently, by Rosenfield et al. (1987). The various radiative heating estimates are consistent with the climatological Antarctic ozone minimum (Hilsenrath and Schlesinger, 1981).

Second, the rapid seasonal development of the ozone hole is difficult to explain by upwelling, unless the vertical velocity significantly exceeds its value in Fig. 4b, c (Solomon, 1987). Therefore, it is doubtful that this dynamical mechanism alone can explain this phenomenon.

## 7. Conclusion

In a geostrophically balanced vortex, the net residual mean meridional circulation is determined by the linear superposition of circulations induced by body forces and diabatic heating. The governing equation is elliptic (except near the equator when cross-equatorial shear is present), and the properties of its analytic, separable solutions remain relevant when realistic mean shear and static stability are used in the numerical solution of (3.4). For vertically localized forcings (into which any distribution of  $D_F$  and  $\bar{Q}^*$  can be decomposed) the streamfunction has a characteristic upward and downward vertical decay scale depending on how the forcing projects onto the eigenfunctions of the latitudinal structure equation. For latitudinally broad forcings, the upward decay scale is much larger than the downward decay scale (Table 1; Plumb, 1982). The upper-tropospheric wavelike driving is a good example of such a latitudinally broad, vertically localized forcing.

Caution is appropriate in applications, since as already stated, the total  $D_F$  is not known. Although an estimate of vertical motion has been obtained from a climatological profile, what really matters in this context are the time variations of  $D_F$  on interannual, seasonal, and day-to-day time scales. The effects of damping will vary greatly over these scales, and it would be premature to make further estimates. Better observational coverage is warranted, in order to evaluate  $D_F$  and its variability more accurately in this region. The radiative and chemical balance must also be understood better. Until further progress is made in all of these areas, a convincing case for a "reverse" residual mean meridional circulation in the Antarctic lower stratosphere cannot be made. Nevertheless, the material discussed in the present paper makes it clear that this region cannot be considered in isolation from neighboring regions, particularly the upper troposphere. The same is of course true of the northern winter stratosphere, except for the quantitative difference that the stratospheric wavelike driving is generally more prominent in this hemisphere, maintaining the polar region well above radiative equilibrium in most winters. Finally, it should be noted that, even if a reverse circulation cell does not exist in the Southern Hemisphere stratosphere, the streamfunction solution depends on the

<sup>1</sup> The climatological Antarctic ozone minimum is consistent with the circulation inferred from the distribution of radiative heating in the Southern Hemisphere lower stratosphere. It is interesting to ask what kinds of body force circulations can explain this differential circulation, with greater subsidence in midlatitudes than at the pole. Within the category of strictly dynamical mechanisms an alternative explanation of the observed departure from radiative equilibrium in midlatitudes might note the role of lateral mixing due to breaking planetary waves (M. E. McIntyre, personal communication, 1987). The effectiveness of this mechanism in the present context will depend on the meridional localization of mixing, i.e., its confinement outside the polar vortex, and the strength of the mixing, dependent on the vertical propagation and breakdown of planetary waves. The relative importance of in situ stratospheric dynamics and nonlocal tropospheric wavelike driving is probably best studied with a series of controlled numerical simulations in which the forcings mechanisms could be specified independently.

distribution of all nearby sources, and the upper-tropospheric waveliving might be of interest, given what is already known about the strength of Southern Hemispheric waveliving and extreme cold temperatures in this region.

*Acknowledgments.* The author thanks M. P. Baldwin, C. R. Mechoso, W. J. Randel, and K. K. Tung for helpful discussions and correspondence. This research was supported by the National Science Foundation, Grant ATM-8616983, and by the National Aeronautics and Space Administration, Contract NASW-4230.

## REFERENCES

- Andrews, D. G., and M. E. McIntyre, 1976: Planetary waves in horizontal and vertical shear: the generalized Eliassen-Palm relation and the mean zonal acceleration. *J. Atmos. Sci.*, **33**, 2031–2048.
- , and —, 1978: Generalized Eliassen-Palm and Charney-Drazin theorems for waves on axisymmetric flows in compressible atmospheres. *J. Atmos. Sci.*, **35**, 175–185.
- , J. D. Mahlman and R. W. Sinclair, 1983: Eliassen-Palm diagnostics of wave-mean flow interaction in the GFDL "SKYHI" general circulation model. *J. Atmos. Sci.*, **40**, 2768–2784.
- Angell, J. K., 1986: The close relation between Antarctic total-ozone depletion and cooling of the Antarctic low stratosphere. *Geophys. Res. Lett.*, **13**, 1240–1243.
- Baldwin, M. P., H. J. Edmon, Jr. and J. R. Holton, 1984: A diagnostic study of eddy, mean-flow interactions during FGGE SOP-1. *J. Atmos. Sci.*, **42**, 1838–1845.
- Barnett, J. J., and M. Corney, 1985a: Middle atmosphere reference model derived from satellite data. *Middle Atmosphere Program, Handbook for MAP*, Vol. 16, K. Labitzke, J. J. Barnett, and B. Edwards, Eds., 318 pp.
- , and —, 1985b: Planetary waves: climatological distribution. *Middle Atmosphere Program, Handbook for MAP*, Vol. 16, K. Labitzke, J. J. Barnett, and B. Edwards, Eds., 318 pp.
- Bojkov, R. D., 1986: The 1979–85 ozone decline in the Antarctic as reflected in ground-based observations. *Geophys. Res. Lett.*, **13**, 1236–1239.
- Bowman, K. P., 1986: Interannual variability of total ozone during the breakdown of the Antarctic circumpolar vortex. *Geophys. Res. Lett.*, **13**, 1193–1196.
- Boyd, J. P., 1976: The noninteraction of waves with the zonally averaged flow on a spherical earth and the interrelationships of eddy fluxes of energy, heat, and momentum. *J. Atmos. Sci.*, **33**, 2285–2291.
- Chubachi, S., 1986: On the cooling of stratospheric temperature at Syowa, Antarctica. *Geophys. Res. Lett.*, **13**, 1221–1223.
- , and R. Kajiwara, 1986: Total ozone variations at Syowa, Antarctica. *Geophys. Res. Lett.*, **13**, 1197–1198.
- Dopplick, T. G., 1979: Radiative heating of the global atmosphere: corrigendum. *J. Atmos. Sci.*, **36**, 1812–1817.
- Dunkerton, T. J., 1978: On the mean meridional mass motions of the stratosphere and mesosphere. *J. Atmos. Sci.*, **35**, 2325–2333.
- , 1987: Resonant excitation of hemispheric barotropic instability in the winter mesosphere. *J. Atmos. Sci.*, **44**, 2237–2251.
- , 1988: Body force circulations in a compressible atmosphere: key concepts. *Pure Appl. Geophys.*, (in press).
- , and D. P. Delisi, 1985: The subtropical mesospheric jet observed by Nimbus 7 LIMS. *J. Geophys. Res.*, **90**, 681–10 692.
- , C.-P. F. Hsu and M. E. McIntyre, 1981: Some Eulerian and Lagrangian diagnostics for a model stratospheric warming. *J. Atmos. Sci.*, **38**, 819–843.
- Edmon, H. J., B. J. Hoskins and M. E. McIntyre, 1980: Eliassen-Palm cross sections for the troposphere. *J. Atmos. Sci.*, **37**, 2600–2616.
- Eliassen, A., 1951: Slow thermally or frictionally controlled meridional circulation in a circular vortex. *Astrophys. Norv.*, **5**, 19–60.
- Farman, J. C., B. G. Gardiner and J. D. Shanklin, 1985: Large losses of total ozone in Antarctica reveal seasonal  $\text{ClO}_x/\text{NO}_x$  interaction. *Nature*, **315**, 207–210.
- Garcia, R. R., 1987: On the mean meridional circulation of the middle atmosphere. *J. Atmos. Sci.*, in press.
- Gardiner, B. G., and J. D. Shanklin, 1986: Recent measurements of Antarctic ozone depletion. *Geophys. Res. Lett.*, **13**, 1199–1201.
- Geisler, J. E., and R. R. Garcia, 1977: Baroclinic instability at long wavelengths on a beta-plane. *J. Atmos. Sci.*, **34**, 311–321.
- Geller, M. A., M.-F. Wu and M. E. Gelman, 1984: Troposphere-stratosphere (surface–55 km) monthly winter general circulation statistics for the Northern Hemisphere—interannual variations. *J. Atmos. Sci.*, **41**, k 1726–1744.
- Hamill, P., O. B. Toon and R. P. Turco, 1986: Characteristics of polar stratospheric clouds during the formation of the Antarctic ozone hole. *Geophys. Res. Lett.*, **13**, 1288–1291.
- Hartmann, D. L., 1976: The structure of the stratosphere in the Southern Hemisphere during late winter 1973 as observed by satellite. *J. Atmos. Sci.*, **33**, 1141–1154.
- , 1983: Barotropic instability of the polar night jet stream. *J. Atmos. Sci.*, **40**, 817–835.
- Hilsenrath, E., and B. M. Schlesinger, 1981: Total ozone seasonal and interannual variations derived from the 7-year Nimbus 4 BUUV dataset. *J. Geophys. Res.*, **86**, 12087–12096.
- Hofmann, D. J., J. W. Harder, S. R. Rolf and J. M. Rosen, 1987: Balloon-borne observations of the development and vertical structure of the Antarctic ozone hole in 1986. *Nature*, **326**, 59–62.
- Holton, J. R., 1975: *The Dynamic Meteorology of the Stratosphere and Mesosphere*. Amer. Meteor. Soc., 319 pp.
- Komhyr, W. D., R. D. Grass and R. K. Leonard, 1986: Total ozone decrease at South Pole, Antarctica, 1964–1985. *Geophys. Res. Lett.*, **13**, 1248–1251.
- Koshelkov, Y. P., 1985: Observed winds and temperatures in the Southern Hemisphere. *Middle Atmosphere Program, Handbook for MAP*, vol. 16, K. Labitzke, J. J. Barnett, and B. Edwards, Eds., 318 pp.
- Labitzke, K., 1981: Stratospheric-mesospheric midwinter disturbances: a summary of observed characteristics. *J. Geophys. Res.*, **86**, 9665–9678.
- Leovy, C. B., 1964: Simple models of thermally driven mesospheric circulations. *J. Atmos. Sci.*, **21**, 327–341.
- , and P. J. Webster, 1976: Stratospheric long waves: comparison of thermal structure in the Northern and Southern Hemispheres. *J. Atmos. Sci.*, **33**, 1624–1638.
- , C.-R. Sun, M. H. Hitchman, E. E. Remsberg, J. M. Russell III, L. L. Gordley, J. C. Gille and L. V. Lyjak, 1985: Transport of ozone in the middle stratosphere: Evidence for planetary wave breaking. *J. Atmos. Sci.*, **42**, 230–244.
- Mahlman, J. D., and S. B. Fels, 1986: Antarctic ozone decreases: a dynamical cause? *Geophys. Res. Lett.*, **13**, 1316–1319.
- , D. G. Andrews, D. L. Hartmann, T. Matsuno and R. G. Murgatroyd, 1984: Transport of trace constituents in the stratosphere. *Dynamics of Middle Atmosphere*. J. R. Holton and T. Matsuno, Eds., Terra Scientific, 387–416.
- Matsuno, T., and K. Nakamura, 1979: The Eulerian and Lagrangian mean meridional circulations in the stratosphere at the time of a sudden warming. *J. Atmos. Sci.*, **36**, 640–654.
- McCormick, M. P., and C. R. Trepte, 1986: SAM II measurements of Antarctica PSCs and aerosols. *Geophys. Res. Lett.*, **13**, 1276–1279.
- Mechoso, C. R., and D. L. Hartmann, 1982: An observational study of traveling planetary waves in the Southern Hemisphere. *J. Atmos. Sci.*, **39**, 1921–1935.
- , D. L. Hartmann and J. D. Farrara, 1985: Climatology and interannual variability of wave, mean-flow interaction in the Southern Hemisphere. *J. Atmos. Sci.*, **42**, 2189–2206.
- Miyahara, S., Y. Hayashi and J. D. Mahlman, 1986: Interactions between gravity waves and planetary-scale flow simulated by

- the GFDL "SKYHI" general circulation model. *J. Atmos. Sci.*, **43**, 1844-1861.
- Nagatani, R. M., and A. J. Miller, 1987: The influence of lower stratospheric forcing on the October Antarctic ozone decrease. *Geophys. Res. Lett.*, **14**, 202-205.
- Newman, P. A., and M. R. Schoeberl, 1986: October Antarctic temperature and total ozone trends from 1979-1985. *Geophys. Res. Lett.*, **13**, 1206-1209.
- Plumb, R. A., 1982: Zonally symmetric Hough modes and meridional circulations in the middle atmosphere. *J. Atmos. Sci.*, **39**, 983-991.
- Rosenfield, J. E., M. R. Schoeberl and M. A. Geller, 1987: A computation of the stratospheric diabatic circulation using an accurate radiative transfer model. *J. Atmos. Sci.*, **44**, 859-876.
- Schoeberl, M. R., A. J. Krueger and P. A. Newman, 1986: The morphology of Antarctic total ozone as seen by TOMS. *Geophys. Res. Lett.*, **13**, 1217-1220.
- Sekiguchi, Y., 1986: Antarctic ozone change correlated to the stratospheric temperature field. *Geophys. Res. Lett.*, **13**, 1202-1205.
- Shiotani, M., and J. C. Gille, 1987: Dynamical factors affecting ozone mixing ratios in the Antarctic lower stratosphere. *J. Geophys. Res.*, **92**, 9811-9824.
- Smith, A. K., 1983: Stationary waves in the winter stratosphere: Seasonal and interannual variability. *J. Atmos. Sci.*, **40**, 245-261.
- Solomon, S., 1987: The mystery of the Antarctic ozone "hole". *Rev. Geophys.*, submitted.
- Stanford, J. L., 1973: Possible sink for stratospheric water vapor at the winter Antarctic pole. *J. Atmos. Sci.*, **30**, 1431-1436.
- , 1977: On the nature of persistent stratospheric clouds in the Antarctic. *Tellus*, **29**, 530-534.
- , and J. S. Davis, 1974: A century of stratospheric cloud reports: 1870-1972. *Bull. Amer. Meteor. Soc.*, **55**, 213-219.
- Stolarski, R. S., and M. R. Schoeberl, 1986: Further interpretation of satellite measurements of Antarctic total ozone. *Geophys. Res. Lett.*, **13**, 1210-1212.
- Straus, D. M., 1981: Long-wave baroclinic instability in the troposphere and stratosphere with spherical geometry. *J. Atmos. Sci.*, **38**, 409-426.
- Tung, K. K., 1982: On the two-dimensional transport of stratospheric trace gases in isentropic coordinates. *J. Atmos. Sci.*, **39**, 2330-2355.
- , 1986: On the relationship between the thermal structure of the stratosphere and the seasonal distribution of ozone. *Geophys. Res. Lett.*, **13**, 1308-1311.
- , M. K. W. Ko, J. M. Rodriguez and N. D. Sze, 1986: Are Antarctic ozone variations a manifestation of dynamics or chemistry? *Nature*, **322**, 811-814.
- Zhang, K.-S., and T. Sasamori, 1985: A linear stability analysis of the stratospheric and mesospheric zonal mean state in winter and summer. *J. Atmos. Sci.*, **42**, 2728-2750.